An explicit PV string model based on the Lambert W function and simplified MPP expressions for operation under partial shading

Efstratios I. Batzelis, *Student Member, IEEE,* Iason A. Routsolias, *Student Member, IEEE,* and Stavros A. Papathanassiou, *Senior Member, IEEE*

***Abstract*— In this paper a reformulation of the widely used one-diode model of the PV cell is introduced, employing the Lambert W function. This leads to an efficient PV string model, where the terminal voltage is expressed as an explicit function of the current, resulting in significantly reduced calculation times and improved robustness of simulation. The model is experimentally validated and then used for studying the operation of PV strings under partial shading conditions. Various shading patterns are investigated, to outline the effect on the string *I-V* and *P-V* characteristics. Simplified formulae are then derived to calculate the Maximum Power Points (MPPs) of a PV string operating under any number of irradiance levels, without resorting to detailed modeling and simulation. Both the explicit model and the simplified expressions are intended for application in shading loss and energy yield calculations.**

***Index Terms*— Explicit model, Lambert W function, Maximum Power Point, Partial shading, PV string, Simplified formulae**

NOMENCLATURE

a	Modified diode ideality factor of the PV cell
a_{bp}	Modified diode ideality factor of the bypass diode
b	Breakdown correction factor of the PV cell
G_j	Irradiance incident on cell strings group j, in per unit (p.u.) of STC value (1000 W/m^2)
I_{mpj}	PV string current at MPPj
I_{ph}	PV cell photocurrent
I_s	PV cell diode saturation current
I_{sbp}	Bypass diode saturation current
$I_{SC,cs}$	PV cell string short circuit current
$MPPj$	Local maximum power point j
N_{cs}	Number of cell strings within each PV module
N_j	Number of cell strings in the group j
N_m	Number of PV modules in the PV string
n	Number of irradiance levels on the PV string
m	Breakdown coefficient of the PV cell
N_s	Number of series-connected cells in each cell string
P_{mpj}	PV string power at MPPj
R_s	Series resistance of the PV cell equivalent circuit
R_{sh}	Shunt resistance of the PV cell equivalent circuit
STC	Standard Test Conditions: Irradiance 1000 W/m^2, Cell temperature 25 °C, Air Mass 1.5
V_{br}	Breakdown voltage of the PV cell
V_{cell}	PV cell voltage
V_{cs}	PV cell string voltage
V_j	Voltage of cell strings group j
V_{mod}	PV module voltage
V_{mp0}, I_{mp0}	PV module MPP voltage and current at STC
V_{mpj}	PV string voltage at MPPj
V_{oc0}	PV module open circuit voltage at STC
V_{str}	PV string voltage
ΔV_D	Voltage drop on a conducting bypass diode
λ	Empirical coefficient for I_{mpj}

Manuscript received January 21, 2013; accepted September 9, 2013. Paper no. TSTE-00024-2013.

Efstratios I. Batzelis was financially supported by PROPONTIS Foundation for this work.

The authors are with the School of Electrical and Computer Engineering, National Technical University of Athens, Athens 15780, Greece (e-mails: batzelis@mail.ntua.gr; iasrouts@mail.ntua.gr; corresponding author: S.A. Papathanassiou, phone: +30 210 7723658, st@power.ece.ntua.gr).

I. Introduction

At non-uniform lighting conditions, parts of the PV generator experience different irradiance, giving rise to multiple local Maximum Power Points (MPPs), which hinder efficient MPP tracking and lead to suboptimal performance.

The standard approach to PV modeling employs the one-diode PV cell electrical equivalent [1]-[2]. Alternative methods for energy yield estimation based on experimental results and empirical formulations are presented in [3]-[5]. These techniques are commonly applied for uniform irradiance conditions, where the PV cell equations can be directly extrapolated to the entire PV generator.

At mismatched operating conditions more sophisticated methods are required, allowing separate modeling of PV cells operating at different illumination levels. In [6], the PV array is modeled by a system of equations numerically solved via the iterative Newton's method. Improvements are reported in [7], presenting a more robust iterative convergence procedure, and in [8] utilizing an artificial neural network for increased execution speed. Related work on changing illumination

conditions is presented in [9] and the development of a reduced system of equations is reported in [10]. Moreover, the use of simplified explicit expressions leading to an optimized method for energy yield estimation is proposed in [11]. A drawback of these methods is computational complexity and convergence issues due to the numerical solution of large systems of equations. In [12], the two-diode PV cell equivalent circuit is implemented in P-Spice to analyze the performance of a single PV module at non-uniform irradiance. In [13], a simple experimental model is proposed for shading effects, presenting moderate accuracy.

In previously published work, the Lambert W function has been utilized to model a single PV cell [14]-[15] or to describe a PV module and form a system of equations for the entire array [16]-[18]. In [19] a single equation is introduced for the PV string, which is iteratively solved to obtain the current for a given voltage. This work assumes uniformly illuminated individual PV modules when analyzing partially shaded arrays and employs a linear approximation for the bypass diodes.

In this paper, an efficient and accurate model, based on the Lambert W function, is presented and applied to analyze the performance of PV module strings under non-uniform irradiance conditions. The model makes use of the Lambert W function to express the PV string voltage as an explicit function of its current, avoiding the need for iterative solution and hence achieving faster and more robust execution. Compared to the model of [19], shading analysis here goes down to the PV cell level, rather than to the level of the PV module, a 4-quadrant *I-V* representation is adopted and the bypass diode is described by its logarithmic equation. The explicit PV string model introduced is suitable for calculations where the *I-V* curve of a PV string needs to be obtained in an efficient and robust manner, as in energy yield calculation and PV array optimization software.

Another core contribution of this paper is the derivation of simple expressions that directly evaluate the MPPs of PV strings, using only module datasheet information. This work expands the concept of [12], which was limited only to PV modules, to the entire PV string. The formulae are derived for the general case of non-uniform shading conditions, where the PV string may experience multiple irradiance levels, giving rise to multiple MPPs on the *P-V* curve. The simplified expressions permit evaluation of shading losses and MPPT effectiveness in shaded conditions in a most simple manner, completely avoiding the need for laborious modeling and simulation.

The structure of the paper is as follows: The explicit PV string model is introduced in Section II and experimentally validated in Section III, using outdoor measurements. The model is then applied in Section IV to analyze the effect of partial shading on PV string performance, for various shading patterns. Simplified expressions which directly provide the MPPs for the general case of multi-peak *P-V* curves are derived in Section V.

II. PV STRING MODELING

A. PV cell electrical equivalent

Various electrical equivalents of the PV cell may be found in the literature, the one-diode model being the most widely used, as it combines simplicity and reasonable accuracy [1], [8]-[10]. The two-diode model described in [6] and [20] provides more accurate results at low irradiance levels, whereas more precise descriptions of PV cell operation at negative voltage are presented in [7], [21]-[26].

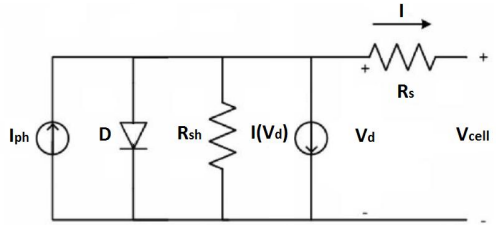

Fig. 1. PV cell electrical equivalent circuit.

In this study, the one-diode model of Fig. 1 is adopted, [1], enhanced by an extension term to represent more accurately the negative diode breakdown operation [7], [22], [25]-[26]. The operation of the PV cell is described by the implicit equation:

$$I = I_{ph} \underbrace{-I_s\left(e^{\frac{V_{cell}+I\cdot R_s}{a}}-1\right)}_{\text{conducting diode modeling}} - \frac{V_{cell}+I\cdot R_s}{R_{sh}} \underbrace{-b(V_{cell}+I\cdot R_s)\left(1-\frac{V_{cell}+I\cdot R_s}{V_{br}}\right)^{-m}}_{\text{negative voltage modeling}} \quad (1)$$

In (1) terms I_{ph}, I_s, a, R_s, R_{sh} are the 5 parameters of the model. Coefficients b, V_{br} and m are important for modeling the operation at negative voltage.

Identification of the 5 parameters is based on the method introduced in [1], first calculating reference (STC) values from datasheet information and then extrapolating to the actual operating conditions. Typical values are assumed for the breakdown terms, close to the values used in [7], [22], [25]: b=0.002Ω^{-1}, V_{br}=-21.29V, m=3.

The *I-V* curve of a PV cell, as calculated by (1), is depicted in Fig. 2. The avalanche breakdown effect at negative voltages is shown, which is of key importance in partial shading analysis.

B. Explicit PV cell model using the Lambert W function

The transcendental form of (1) leads to *I-V* calculation through iterative numerical procedures, such as Newton's method. Modeling of larger PV structures is achieved by forming a system of equations, in which each cell is separately described by a single equation [6]-[9], [11]. However, when reaching the level of entire PV strings or arrays, the resulting equation system tends to become prohibitively large, imposing a heavy computational burden and raising convergence issues. To circumvent this problem, an alternative approach is employed, where the base equation of the PV cell is expressed in an explicit form $V=f(I)$. In the next section, this approach is

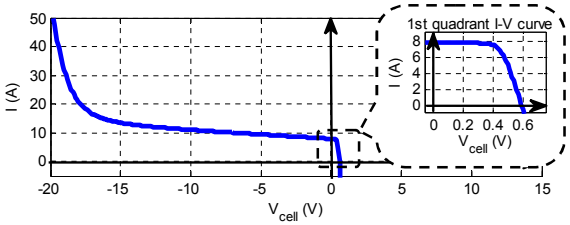

Fig. 2. 4-quadrant *I-V* curve of a typical PV cell.

extended to PV modules and then to the level of PV strings.

Eq. (1) can be simplified by observing that, at negative voltages, the exponential term of the conducting diode reaches near-zero values as diode D is reverse biased. Further, at positive voltages, the last term in (1), modeling the avalanche breakdown effect, has no practical significance. Therefore, the base PV cell equation can be modified as follows, employing simplified expressions for each operating region:

$$I=\begin{cases} I_{ph}-I_s\left(e^{\frac{V_{cell}+I\cdot R_s}{a}}-1\right)-\dfrac{V_{cell}+I\cdot R_s}{R_{sh}} & ,V_{cell}\geq 0\ (I\leq I_{ph}) \\ I_{ph}-\dfrac{V_{cell}+I\cdot R_s}{R_{sh}}-b(V_{cell}+I\cdot R_s)\left(1-\dfrac{V_{cell}+I\cdot R_s}{V_{br}}\right)^{-m} & ,V_{cell}<0\ (I>I_{ph}) \end{cases} \quad (2)$$

At positive voltages, (2) is identical to the typical equation of the standard one-diode model, which can be solved for the voltage using the Lambert W function:

$$V_{cell}=R_{sh}\cdot(I_{ph}+I_s)-(R_s+R_{sh})\cdot I-a\cdot W\left\{\frac{R_{sh}I_s}{a}e^{\frac{R_{sh}\cdot(I_{ph}+I_s-I)}{a}}\right\} \quad (3)$$

where the series expansion approximations employed here for evaluating $W\{x\}$ are given in the Appendix.

At negative voltages, (2) may be transformed to a quartic equation, if the typical value m=3 is assumed [7], [22], [25]:

$$\frac{1}{R_{sh}}\cdot z^4+\left(I_{ph}-I-\frac{V_{br}}{R_{sh}}\right)\cdot z^3+bV_{br}^3\cdot z-bV_{br}^4=0 \quad (4)$$

where $z=V_{br}-V_{cell}-I\cdot R_s$.

The PV cell voltage V_{cell} is then given by the minimum real root of the polynomial equation (4), $z_{Rmin}=\min\{\text{real}\{z\}\}$, which can be obtained by application of the fast and robust Ferrari's method for solving quartic equations [27]-[28]. Although m=3 is often considered [7], [22], [25], a wider range of m values, between 3 and 6, is also suggested [21], [23]-[24], [26]. In such a case, (4) turns into a polynomial equation of higher degree, which can be numerically solved, although not as efficiently as using the explicit formula of Ferrari.

Finally, (5) below constitutes the explicit expression for evaluating the PV cell voltage as a function of its current:

$$V_{cell}=\begin{cases} R_{sh}\cdot(I_{ph}+I_s)-(R_s+R_{sh})\cdot I-a\cdot W\left\{\dfrac{R_{sh}I_s}{a}e^{\frac{R_{sh}\cdot(I_{ph}+I_s-I)}{a}}\right\} & ,I\leq I_{ph} \\ V_{br}-I\cdot R_s-z_{R\min} & ,I>I_{ph} \end{cases} \quad (5)$$

C. Explicit model for PV strings

In PV modules, bypass diodes are connected in parallel to groups of series-connected PV cells, to prevent development of high negative voltages on the cells and hot-spot phenomena. In this way, *cell strings* are formed, consisting of N_s series-connected PV cells (e.g. as in Fig. 7). The bypass diode conducts only at negative voltages, effectively shorting the cell string terminals, whose voltage is thus clipped to the forward voltage drop of the diode (typically around 0.7 V).

A typical cell string *I-V* characteristic is shown in Fig. 3, with and without a bypass diode. The latter has an impact only at negative voltages, where the cell string *I-V* curve effectively becomes that of the conducting diode. To determine V_{cs} in this

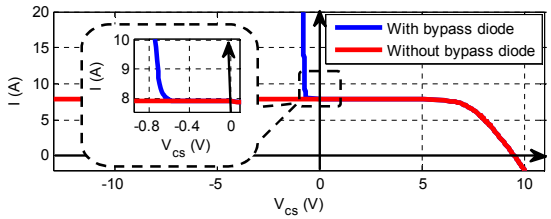

Fig. 3. *I-V* curve of a PV cell string with and without a bypass diode.

operating region (approximately -0.7 to 0 V), the bypass diode equation can be used, observing that the cell string itself (red line in Fig. 3) operates at practically constant current, equal to its short circuit current $I_{SC,cs}$, and therefore the diode carries the difference of the total current I minus $I_{SC,cs}$. Hence, given the cell string current I, its voltage V_{cs} may be calculated from:

$$V_{cs}=\begin{cases} \sum_{i=1}^{Ns}V_{cell-i}(I) & ,I\leq I_{SC,cs} \\ -a_{bp}\cdot\ln\left(\dfrac{I-I_{SC,cs}}{I_{sbp}}+1\right) & ,I>I_{SC,cs} \end{cases} \quad (6)$$

In the first and fourth quadrant, the cell string voltage is simply the sum of the individual cell voltages, V_{cell-i}, given by (5). In the second quadrant, $I_{SC,cs}$ may be taken equal to the minimum short circuit current of the individual cells in the string, approximated by the respective photocurrents.

A PV module, composed by a number of N_{cs} cell strings connected in series, is described by:

$$V_{\text{mod}}=\sum_{i=1}^{N_{cs}}V_{cs-i}(I) \quad (7)$$

and a PV string consisting of N_m modules connected in series:

$$V_{str}=\sum_{i=1}^{Nm}V_{\text{mod}-i}(I) \quad (8)$$

Eqs. (5)-(8) constitute the explicit model of the PV string, giving in a straightforward manner its voltage as a function of its current, without any need for iterative procedures.

At this point it is essential to highlight similarities and differences of this approach with previous relevant studies. In [16]-[17] the Lambert W function is used to describe the PV module and form a system of equations for the PV array, numerically solvable by Newton's method. An improvement is reported in [18], where the inverse Jacobian matrix is explicitly determined. These methods do not overcome the computational burden of an iterative solution procedure.

In [19], the Lambert W function is used to express the PV string voltage as an explicit function of the current. The PV module constitutes the basic building block (since uniformly illuminated individual PV modules are assumed at partial array shading) and a simplified bypass diode representation is adopted, consisting of a voltage source and a series resistor. Further, a numerical solution is still employed in the implementation of the model, as the voltage is selected to be the independent variable. On the other hand, the model introduced here goes down to the cell level, describing operation at negative voltages, which is important in partial shading conditions, while the fundamental bypass diode equation is used, without any simplification. In this way, the partial shading of individual modules is appropriately modeled

and the effect of bypass diodes is more accurately described. Since the model is intended for energy yield calculations and PV system analysis, involving calculation of the *I-V* characteristic, the current is used as the independent variable, obviating the need for an iterative solution.

The PV string model presented above provides also the basis for addressing PV arrays consisting of several PV strings connected in parallel. Two alternative approaches are possible in this case: predetermination of the *I-V* curve of each string and graphical superposition of the individual curves to construct the array *I-V* characteristic, as in [10], or iterative solution of each string's equations for a given terminal voltage and then summation of the individual currents, as in [19].

In the first approach, the proposed PV string model is utilized to calculate explicitly the *I-V* curve for each string, using a suitably selected vector of string currents as input variable. Thereafter, the *I-V* curves of the individual strings are summed using a common voltage axis and linear interpolation is applied to identify any particular operating point of the array on the curve. Although the superposition procedure involves calculation of multiple operating points on the *I-V* curve, it introduces negligible computation burden, since it employs simple algebraic operations.

The second approach involves the numerical solution of eq. (8) for each PV string, at a given terminal voltage, using an iterative method, such as Newton's, in order to determine the resulting string current value. PV string currents are then summed to obtain the total current of the array. This method suffers from the computational cost of an iterative solution procedure and the related convergence issues. Still, its application is feasible and appealing as only a small number of independent equations needs to be solved (one per string).

D. Comparison of standard and explicit models

The explicit PV string model overcomes the shortcomings of the standard PV cell modeling approach, permitting efficient calculation, without convergence issues, initialization difficulties and other numerical inefficiencies. The "standard model" used as a reference here is the equation system derived by applying (1) for all cells. This can be numerically solved, e.g. by the Newton's method with appropriate optimization (efficient initialization strategy, predetermination of Jacobian matrix etc.).

The gain in computational effort is demonstrated in Fig. 4. The diagram shows the ratio of the execution time required to determine the *I-V* characteristic of a PV string using the standard model to that using this paper's model, against the total number of cells in the PV string. For a practical string, comprising 600-1000 PV cells, a reduction of 2-3 orders of magnitude can be achieved using the proposed explicit model.

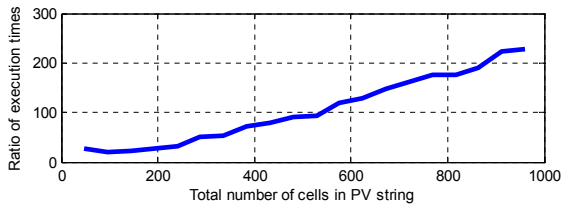

Fig. 4. Ratio of execution times of the standard model to that of the explicit model, as a function of the number of cells in the PV string.

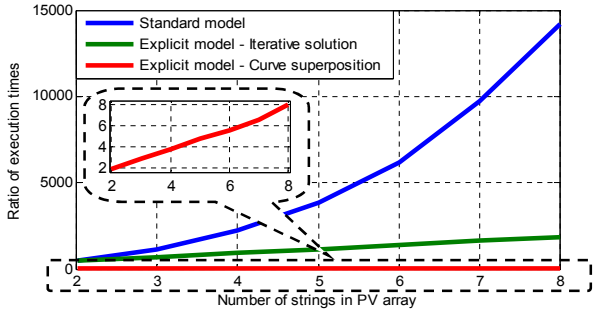

Fig. 5. Time required to calculate the *I-V* characteristic of a PV array vs. the number of strings in the array, using the standard model and the two proposed approaches. Execution times are normalized on the time required to simulate a single PV string by the explicit model.

In Fig. 5 a similar comparison is shown for the case of a PV array, using either the standard model or the two alternative approaches proposed in the previous section. Assuming strings of 20 PV modules (960 cells) each, the *I-V* curve of an array comprising 2-10 strings in parallel is calculated (at 100 discrete points). To facilitate comparison, the computational burden is normalized on the time required by the explicit model to perform the *I-V* curve calculation of a single string. As expected, the standard model (blue line) exhibits an exponential increase of the computational cost with the number of strings, as the system of equations tends to become oversized. The curve superposition approach (red line) presents a proportional dependence on the number of strings, as the computational cost is practically associated only with the determination of the *I-V* curve of each individual string. The method of solving the explicit equations of the strings also presents a burden proportional to the size of the array. This cost is greater than for the curve superposition method, as the individual PV string equations need to be solved iteratively, but still remains low compared to the standard model (linear instead of exponential increase of the burden).

In terms of accuracy, modeling the PV cell by (2) yields almost identical results compared to the fundamental eq. (1), the error being lower than 0.1%. The number of terms chosen for the Lambert W series (see Appendix) is sufficient and the separation of (1) in two branches using I_{ph} as the inflection point is justified. At extreme shading conditions, such as when 1 cell out of 16 is heavily shaded at an irradiance level of G=0.1 p.u. (while G=1.0 p.u. is considered for the unshaded part), as shown in Fig. 6, the explicit model may deviate slightly at negative voltages, due to the $I_{SC,cs}$ estimation used in the second branch of (6). The difference is noticeable on the

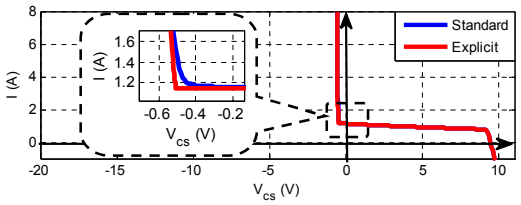

Fig. 6. *I-V* curve of a PV cell string, when 1 cell out of 16 is heavily shaded at G=0.1 p.u., using the standard and the explicit model.

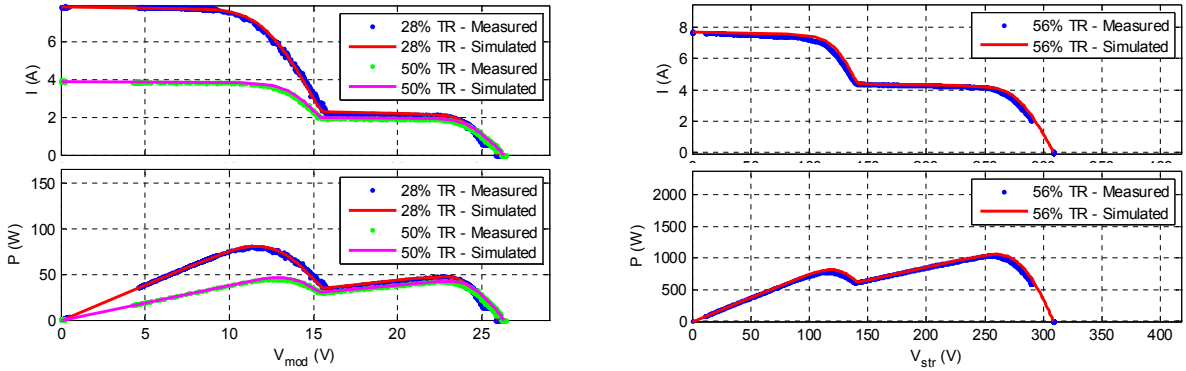

(a) PV module - 2 cell rows shaded (2 measurements sets) (b) PV string - 8 modules shaded by 4 cell rows each

Fig. 8. Experimental and simulated *I-V* and *P-V* curves of a partially shaded (a) PV module and (b) PV string.

diagram but has no significant effect on the application of the model, since it corresponds to the local minima of the *P-V* curve.

III. Experimental Validation of the Model

The model introduced in Section II is experimentally validated for a single PV module and a string of modules. For this purpose, outdoor measurements were taken at a string of commercial PV modules operating at different irradiance levels and shading patterns. The datasheet characteristics of the modules are shown in Table I and the physical layout of the cells in Fig. 7. Three cell strings are formed, of 16 cells each. The model parameters for the PV cell at STC are presented in Table II. The reference values of the 5 parameters I_{ph}, I_s, a, R_s, R_{sh} are extracted from the module datasheet characteristics and then extrapolated to the actual operating conditions according to [1]. For the breakdown terms b, V_{br}, m typical constant values are assumed, similar to those in [7], [22], [25]. The bypass diode coefficients I_{sbp} and a_{bp} are based on [7]-[8], adjusted by laboratory measurements of the *I-V* curve of the diodes.

TABLE I
Experimental PV Module Datasheet Characteristics

Model	Type	N_s	N_{cs}	I_{sc0} (A)	V_{oc0} (V)	I_{mp0} (A)	V_{mp0} (V)
Yingli YL-165	mc-Si	16	3	7.90	29.0	7.20	23.0

TABLE II
Cell Parameters for the Experimental PV Module at STC

I_{ph}(A)	I_s(A)	a(V)	R_s(Ω)	R_{sh}(Ω)	b(Ω^{-1})	V_{br}(V)	m	I_{sbp}(A)	a_{bp}(V)
7.93	3.8e-10	0.025	0.013	3.3	0.002	-21.93	3	1.6e-9	0.05

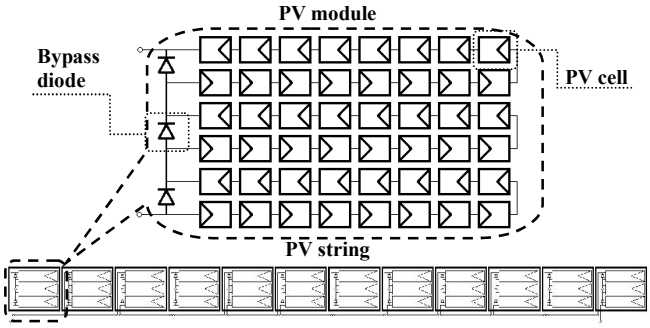

Fig. 7. Layout of the PV module and string used in the measurements.

The *I-V* curve of the module was recorded at two different irradiance levels, while shading patterns were generated using shading materials with transmittance rates (*TR*) of 28% and 50%. In Fig. 8(a), the measured and calculated *I-V* and *P-V* characteristics of the PV module are shown for an indicative partial shading scenario (2 cell rows, i.e. 1/3 of the module area) at two operating conditions: G=0.98 p.u./T_c=48°C and G=0.49 p.u./T_c=39°C respectively. The efficiency of the model in representing the actual PV module characteristic is satisfactory over the entire range of the *I-V* curves and for all shading scenarios. This is further confirmed in Table III, where the MPP power calculation error is presented for several shading scenarios.

A similar procedure was followed to validate the accuracy of the model in the case of PV strings. A string consisting of 12 series-connected identical PV modules was used, (Fig. 7) whose characteristics are given in Table I and measurements were taken at several operating conditions. Indicative results are presented in Fig. 8(b), for a case where 8 modules are partially shaded over 2/3 of their surface (4 cell rows each) using a shading material with *TR*=56% at G=0.97 p.u./T_c=52°C. Results for different shading patterns of the PV string are summarized in Table III.

IV. PV String Operation Under Partial Shading

The purpose of this section is to illustrate the response of a PV string when it is partially shaded. To facilitate

TABLE III
MPP Calculation Error of the Explicit Model Compared to Measurements

PV module			PV string	
Shading scenario	MPP error (%) Series #1 (*TR*=28%)	MPP error (%) Series #2 (*TR*=50%)	Shading scenario	MPP error (%) (*TR*=56%)
Unshaded	0.67	0.93	Unshaded	2.53
1 row shade	4.18	1.02	2 rows shade	2.16
2 rows shade	0.88	1.85	4 rows shade	0.79
4 rows shade	0.68	3.62	1 module shade	2.88
1 column shade	0.73	1.25	6 modules shade	3.24
4 columns shade	1.05	2.36	1 cell string shade	3.37
3x2 cells shade	3.07	0.31	8 modules by 4 rows each shade	1.70
Full shade	2.55	0.48		

understanding of the phenomenon, first the simplified case of two irradiance levels (corresponding to the shaded and unshaded areas) is analyzed, where only two MPPs appear on the *P-V* characteristic. Then, the observations made are extended to the general case of *n* irradiance levels, where up to *n* MPPs may appear.

A. PV cell

The PV cell is the elementary building block of a PV string and its operation is described by (1). The irradiance level affects linearly the short circuit current and logarithmically the open circuit voltage [4], [22]. In Fig. 9(a), the effect of the incident irradiance on the *I-V* curve of one cell is shown for the PV module under study.

B. PV cell string

Since all cells in a cell string carry the same current, at partial shading conditions the unshaded cells operate at reduced current, restricted by the short circuit current of the shaded cells. In Fig. 9(b) a cell string (16 cells) of the study - case PV module is simulated for an increasing number of shaded cells. The irradiance on the unshaded and shaded parts is G_1=1.0 p.u. and G_2=0.5 p.u., respectively. Even for a minimum number of shaded cells, the *I-V* curve of the partially shaded cell string approaches that of the fully shaded string. This well-known fact [8], [22] is a common modeling simplification.

C. PV module

The operation of a PV module in partial shading conditions has been extensively investigated in [12]. Fig. 10(a) presents the response of the study-case PV module for an increasing number of shaded cells. Assuming 2 levels of irradiance on the module, the module *P-V* curve presents 2 local maxima, MPP1 and MPP2, and 2 groups of cell strings are formed, group 1 (unshaded) and group 2 (shaded), illuminated at G_1=1.0 p.u. and G_2=0.5 p.u. respectively. Around MPP1 the shaded cell strings (group 2) are bypassed and only the unshaded ones (group 1) generate power, whereas at the MPP2 region all cell strings contribute to power generation at reduced current.

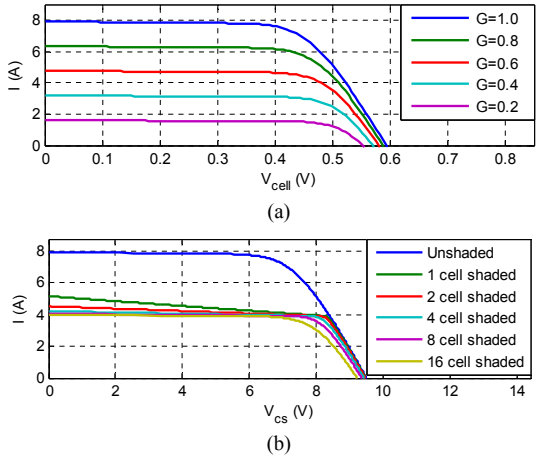

Fig. 9. *I-V* curves of a shaded (a) PV cell at different irradiance levels and (b) PV cell string for different number of shaded cells (G_1=1.0 p.u., G_2=0.5 p.u.).

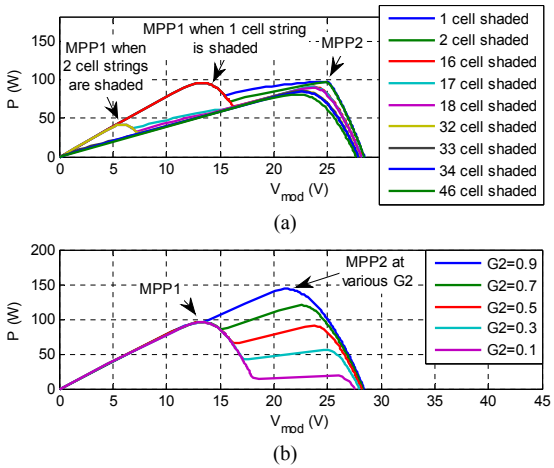

Fig. 10. *P-V* curves of a shaded PV module for (a) different number of shaded cells (G_1=1.0 p.u., G_2=0.5 p.u.) and (b) different irradiance level on the shaded part G_2 (1 cell string shaded).

When only one cell string experiences shading of various degrees (1-16 cells shaded), the corresponding curves do not deviate significantly from each other, since the partially shaded cell string operates approximately as a fully shaded one. When 17-32 cells are shaded, MPP1 is shifted to lower voltages, since only N_1=1 cell string is unshaded, while the remaining N_2=2 cell strings are bypassed. However, when all 3 cell strings are shaded, MPP1 is completely suppressed because none of the bypass diodes conducts and the *P-V* characteristic is dominated by the series-connected shaded cell strings. MPP2 remains little affected in any of the above cases.

In Fig. 10(b) one cell string of the PV module is fully shaded (N_2=1) at various intensities G_2, while the other two operate unshaded (N_1=2, G_1=1.0 p.u.). In all cases, MPP1 is unaffected since the shaded cell string is bypassed, while MPP2 is affected by the changing irradiance levels G_2.

In conclusion, a PV module operating under non-uniform lighting conditions typically presents 2 maxima on its *P-V* curve, if one level of shade is considered. The first (MPP1) is primarily affected by the number of unshaded cell strings N_1, while the second (MPP2) mainly depends on the irradiance G_2 on the shaded part.

D. PV string

From a modeling point of view, a PV string can be treated as an oversized PV module, comprising several series-connected cell strings. In this section, the 12-module PV string of Fig. 7 is simulated, both in landscape and portrait orientation, considering several realistic shading scenarios and assuming one level of shade. Typical patterns along with the resulting *P-V* curves are shown in Fig. 11.

A first observation is the appearance of 2 local maxima (corresponding to MPP1 and MPP2 of Fig. 10), following similar trends as for the single PV module. This is reasonable, because the PV string is composed by unshaded and (partially or fully) shaded groups of cell strings connected in series and its response depends on the number of cell strings in each group, regardless of their location within the string and the number of shaded cells within each cell string.

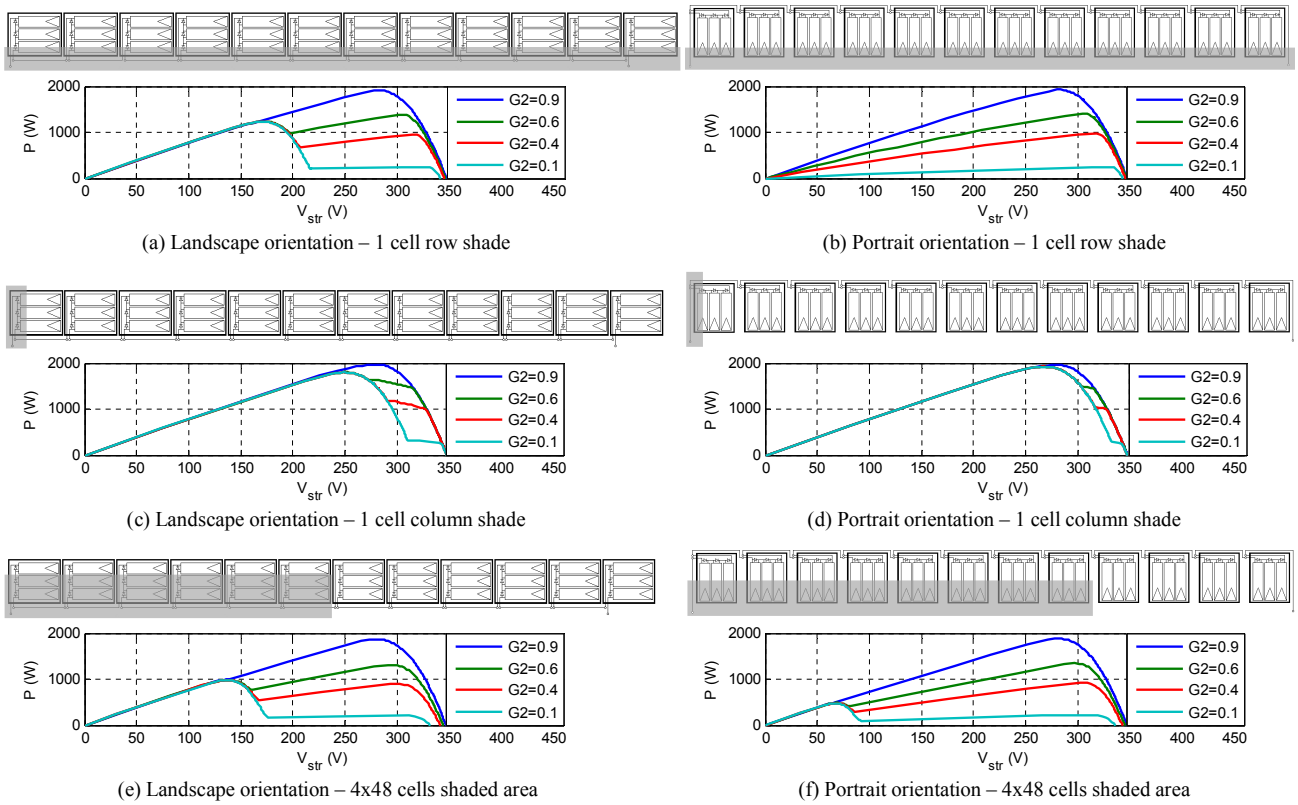

(a) Landscape orientation – 1 cell row shade

(b) Portrait orientation – 1 cell row shade

(c) Landscape orientation – 1 cell column shade

(d) Portrait orientation – 1 cell column shade

(e) Landscape orientation – 4x48 cells shaded area

(f) Portrait orientation – 4x48 cells shaded area

Fig. 11. *P-V* curves of a partially shaded PV string in landscape and portrait orientation at typical shading scenarios (one level of shade).

In Fig. 11(a)-(b) a shadow pattern most commonly encountered in practice is shown. It affects one cell row at the bottom of all modules, impacting thus only 12 cell strings when in landscape mode, but all 36 cell strings in portrait orientation, in which case MPP1 is entirely suppressed. This will lead to reduced overall performance at deep levels of shadow (G_2<0.5 p.u.), provided that MPP operation is possible at the substantially reduced voltages near MPP1. On the other hand, the portrait mode is slightly less sensitive to lateral shading, as in Fig. 11(c)-(d), because the shadow expands cell string-by-cell string, rather than module-by-module as in the landscape mode. For diagonal shadow patterns, as shown in Fig. 11(e)-(f), more partially shaded cell strings exist in portrait. In conclusion, the landscape orientation is slightly less susceptible to shadow effects in most practical situations.

The *P-V* curves of a PV string subject to two irradiance levels present up to 2 local MPPs, regardless of the shade level or pattern, since the exact location of the shaded cell strings along the entire series-connected chain does not matter. Hence, two MPPs are also observed when a PV string extends to more than one rows, a situation common in installations where the length of the arrays is limited.

E. Partial shading at n irradiance levels

Although the assumption of one level of shade is common, in the general case a partially shaded PV string may be subjected to several different irradiance levels. This situation might occur when different objects cast shadows on the array (e.g. an adjacent array and a solid object at a greater distance), giving rise to more than two MPPs on the *P-V* curve.

In Fig. 12, an indicative scenario of a PV string illuminated at three irradiance levels, G_1, G_2 and G_3, is depicted. The respective cell string groups comprise N_1=18, N_2=6 and N_3=12 cell strings.

In this case, 3 MPPs are presented on the *P-V* curve. At MPP1 only group 1 generates power, while groups 2 and 3 are bypassed. At MPP2 groups 1 and 2 contribute to power generation at the reduced current determined by G_2, while group 3 is bypassed. At MPP3 all three groups generate power at the lowest current imposed by the least illuminated group 3.

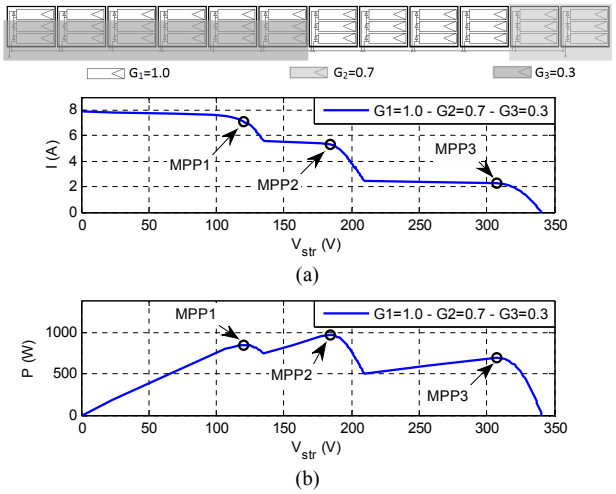

(a)

(b)

Fig. 12. Indicative case of a partially shaded PV string, illuminated at three irradiance levels (G_1=1.0 p.u., G_2=0.7 p.u., G_3=0.3 p.u.).

These observations are readily generalized to a PV string illuminated at n irradiance levels G_j, j=1..n, sorted in decreasing order (G_i>G_j, i>j). Then, n local MPPs may appear on the P-V curve of the string, provided that a sufficient number (≥n) of bypass diodes exists, a condition implicitly assumed to be valid in the following. At MPPj, cell string groups j+1 to n are shorted by the respective bypass diodes, while groups 1 to j operate at the current dictated by the irradiance level G_j, incident on group j. Thus, a conceptual association can be established between each local MPPj and the irradiance level G_j on group j, comprising N_j cell strings.

V. Simplified Formulae for Direct Determination of MPPs in Partially Shaded PV Strings

In this section, simple expressions are derived to evaluate the voltage and current of the MPPs of a partially shaded PV string, using only PV module datasheet information and completely avoiding the modeling required in order to derive the P-V characteristics of the entire string. In Section V.A the simplified case of one shade level is first analyzed in detail, to provide the basis for generalization to n irradiance levels in Section V.B.

A similar analysis has been performed in [12], however only for the case of a single PV module, rather than a string. Further, the granularity of the modeling approach in [12] is too fine, extending down to the PV cell level, which is not practical when dealing with entire PV strings or arrays.

To derive the equations in the following, cell temperature changes are ignored (all cells operate at 25 °C). Since the performance of partially and fully shaded cell strings is similar, the effect of shadow on the operation of the entire PV string depends on the number of irradiance levels n and their intensities G_j, j=1..n, as well as the number N_j of cell strings in each group j. The exact geometric shape of the shadow does not have any significance.

A. Simplified expressions for two irradiance levels

In this case, two groups of cell strings are formed, comprising N_1 and N_2 cell strings, that operate at irradiance levels G_1 and G_2 (unshaded and shaded part, respectively). As discussed in Section IV, at MPP1 the shaded cell strings are bypassed and the equivalent circuit of the PV string consists of N_1 unshaded cell strings connected in series to N_2 conducting bypass diodes. Hence, the following equation, reformulated from [12], gives the voltage, V_{mp1}, of MPP1:

$$V_{mp1} = N_1 \frac{V_{mp0}}{N_{cs}} - N_2 \Delta V_D \tag{9}$$

where V_{mp0}/N_{cs} is the MPP voltage of a single unshaded cell string, which depends very little on the irradiance, and ΔV_D is the voltage drop across a bypass diode (typically 0.7-1.0 V).

The current at MPP1 is considered to be directly proportional to the irradiance G_1 of the unshaded group:

$$I_{mp1} = G_1 I_{mp0} \tag{10}$$

In Fig. 13, the dependence of V_{mp1}, I_{mp1} and P_{mp1} on N_2 and G_2 is illustrated for the study-case PV string (considering G_1=1.0 p.u. on the unshaded group). Continuous lines

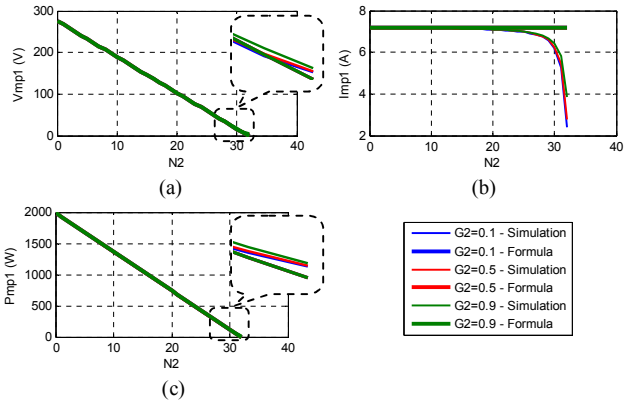

Fig. 13. (a) V_{mp1}, (b) I_{mp1} and (c) P_{mp1} dependence on the number of shaded cell strings (N_2) and the irradiance on the shaded part (G_2) for the study-case PV string (G_1=1.0 p.u.).

represent simulation results obtained with the explicit model, while dotted lines are obtained with the simplified expressions. From Fig. 13 it is clear that the MPP1 is indeed rather independent of the irradiance on the shaded part G_2, while V_{mp1} appears to vary linearly with N_2 (and therefore N_1, as well), as assumed in (9). Eq. (10) provides a satisfactory estimate of I_{mp1}, except when too many cell strings are shaded. Then, I_{mp1} decreases because of the accumulated voltage drop on the conducting bypass diodes, which effectively alters the I-V curve and shifts MPP1 to larger voltages and lower currents (Figs. 13(a), (b)). However, the errors in V_{mp1} and I_{mp1} at large values of N_2 tend to counterbalance each other, resulting in an accurate enough evaluation of P_{mp1} over the entire range of N_2 (Fig. 13(c)). In any case, MPP1 is not important under extended shading, as the P-V curve is typically dominated by MPP2. Actually, there is a critical value of N_2 (N_2=32 in Fig. 13) above which MPP1 does not exist, because the unshaded cell strings cannot "overcome" the voltage drop on the conducting bypass diodes.

In the MPP2 region, all cell strings participate in power generation, operating at the reduced current imposed by the shaded ones. In this case, the PV string voltage V_{mp2} is the sum of the voltages of all cell strings:

$$V_{mp2} = N_1 V_1 + N_2 V_2 \tag{11}$$

The voltage V_2 of each shaded cell string is assumed to be equal to its MPP voltage, V_{mp0}/N_{cs}, and independent of the irradiance G_2, as mentioned previously.

The voltage V_1 of the unshaded cell strings is estimated via a linear approximation, as illustrated in Fig. 14. The actual I-V curve of each unshaded cell string (continuous blue line) is approximated in the MPP2 region by a straight line (dotted blue line), passing through the MPP and open circuit points:

$$V = \frac{V_{mp0} - V_{oc0}}{N_{cs} G_1 I_{mp0}} I + \frac{V_{oc0}}{N_{cs}} \tag{12}$$

where the MPP and open circuit voltages are assumed to be independent of the incident irradiance G_1, while the MPP current is directly proportional to G_1. Considering I_{mp2} at MPP2 to be also proportional to the irradiance G_2 on the shaded group, $G_2 \cdot I_{mp0}$, V_1 is then given by the intersection of the blue and green dotted lines by setting I=$G_2 \cdot I_{mp0}$ in (12):

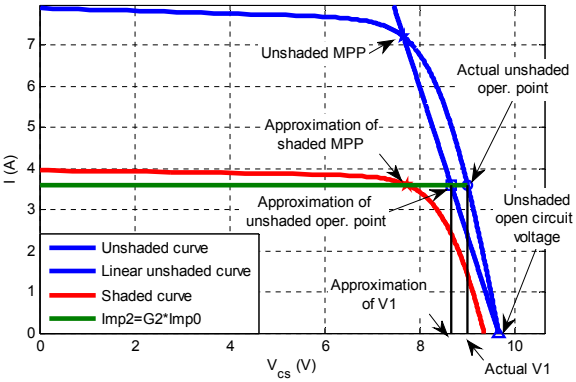

Fig. 14. Approximation of unshaded cell string voltage, V_1, at MPP2.

$$V_1 = \frac{V_{mp0} - V_{oc0}}{N_{cs} G_1 I_{mp0}} G_2 I_{mp0} + \frac{V_{oc0}}{N_{cs}} \Leftrightarrow V_1 = \frac{G_2}{G_1}\frac{V_{mp0}}{N_{cs}} + (1 - \frac{G_2}{G_1})\frac{V_{oc0}}{N_{cs}} \quad (13)$$

Hence, the complete expression for V_{mp2} becomes:

$$V_{mp2} = N_1\left(\frac{G_2}{G_1}\frac{V_{mp0}}{N_{cs}} + (1 - \frac{G_2}{G_1})\frac{V_{oc0}}{N_{cs}}\right) + N_2\frac{V_{mp0}}{N_{cs}} \quad (14)$$

Moreover, extensive simulations showed I_{mp2} to be directly proportional to G_2 and to vary linearly with the number of unshaded cell strings N_1, leading to the following expression:

$$I_{mp2} = G_2 I_{mp0}\left(1 + \lambda\frac{N_1}{N_m N_{cs}}\right) \quad (15)$$

where the empirical coefficient λ, estimated via regression on the simulation results for several commercial mono-crystalline (c-Si) and multi-crystalline (mc-Si) PV modules, presents small variance, leading to the adoption of λ=0.06 as a typical value.

The dependence of MPP2 on N_2 and G_2 is depicted in Fig. 15. While the V_{mp2} estimation is of moderate accuracy at small values of G_2, the approximation of I_{mp2} is satisfactory, leading to a fairly accurate evaluation of P_{mp2}.

The final expressions which permit direct evaluation of the MPP1 and MPP2 voltages and currents of a partially shaded PV string at two irradiance levels are the following:

$$MPP1: \begin{cases} V_{mp1} = N_1\frac{V_{mp0}}{N_{cs}} - N_2\Delta V_D & (16a) \\ I_{mp1} = G_1 I_{mp0} & (16b) \end{cases}$$

$$MPP2: \begin{cases} V_{mp2} = N_1\left(\frac{G_2}{G_1}\frac{V_{mp0}}{N_{cs}} + (1 - \frac{G_2}{G_1})\frac{V_{oc0}}{N_{cs}}\right) + N_2\frac{V_{mp0}}{N_{cs}} & (16c) \\ I_{mp2} = G_2 I_{mp0}\left(1 + \lambda\frac{N_1}{N_m N_{cs}}\right) & (16d) \end{cases}$$

$$Global\ MPP: P_{mp} = \max\left\{P_{mp1} = V_{mp1}I_{mp1}, P_{mp2} = V_{mp2}I_{mp2}\right\} \quad (16e)$$

B. *Generalized expressions for n irradiance levels*

In the general case, the PV string may be subjected to more than two irradiance levels, giving rise to several MPPs on the *P-V* curve, as discussed in Section IV.E. In Fig. 16, a simplified example is shown of a PV string comprising four cell strings illuminated at different irradiance levels (i.e. 1 cell string per group). The resulting *P-V* curve presents four MPPs, associated with the operation of the individual cell strings as explained in Section IV.E. E.g. at MPP3 cell strings 1-3 operate at the reduced current I_{mp3}, dictated by the irradiance

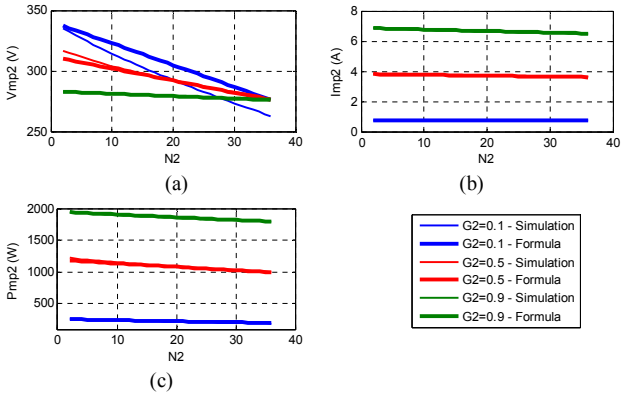

Fig. 15. (a) V_{mp2}, (b) I_{mp2} and (c) P_{mp2} dependence on the number of shaded cell strings (N_2) and on the shaded part (G_2) for the study-case PV string (G_1=1.0 p.u.).

level G_3 of group 3, while group 4 is bypassed. The voltage V_{mp3} is the sum of the voltages V_j of the component cell strings. Since groups 1 and 2 operate at reduced current, V_1 and V_2 may be estimated by a linear approximation similar to eq. (13). Group 3 operates at $V_3 = V_{mp0}/N_{cs}$, while the bypassed group 4 contributes the voltage drop on its bypass diode, ΔV_D. Hence:

$$V_{mp3} = \underbrace{N_1\left(\frac{G_3}{G_1}\frac{V_{mp0}}{N_{cs}} + (1 - \frac{G_3}{G_1})\frac{V_{oc0}}{N_{cs}}\right)}_{V1} + \underbrace{N_2\left(\frac{G_3}{G_2}\frac{V_{mp0}}{N_{cs}} + (1 - \frac{G_3}{G_2})\frac{V_{oc0}}{N_{cs}}\right)}_{V2} + \underbrace{N_3\frac{V_{mp0}}{N_{cs}}}_{V3} - \underbrace{N_4\Delta V_D}_{V4} \quad (17)$$

The concept of eq. (15) is directly extended to provide I_{mp3}, which varies in direct proportion to the irradiance G_3 and depends to a small extent on the number of cell strings in groups 1 and 2:

$$I_{mp3} = G_3 I_{mp0}\left(1 + \lambda\frac{N_1 + N_2}{N_m N_{cs}}\right) \quad (18)$$

Following this line of thought, the final expressions for the MPPs in the general case of n irradiance levels are readily derived. For MPPj (j=1..n):

$$MPP_j: \begin{cases} V_{mpj} = \sum_{i=1}^{j} N_i\left[\frac{G_j}{G_i}\frac{V_{mp0}}{N_{cs}} + \left(1 - \frac{G_j}{G_i}\right)\frac{V_{oc0}}{N_{cs}}\right] - \sum_{i=j+1}^{n} N_i\Delta V_D & (19a) \\ I_{mpj} = G_j I_{mp0}\left[1 + \lambda\frac{\sum_{i=1}^{j-1} N_i}{N_m N_{cs}}\right] & (19b) \\ P_{mpj} = V_{mpj} I_{mpj} & (19c) \end{cases}$$

V_{mpj} in eq. (19a) is the sum of the linearly approximated voltage contributions of the j-1 groups with higher incident irradiances, plus the MPP voltage of group j, minus the voltage drops on the bypass diodes of the remaining n-j groups, which are illuminated less than group j. Eq. (19b) reflects the predominant dependence of I_{mpj} on the irradiance level G_j on group j, along with the secondary effect of the j-1 groups, which are more illuminated than group j.

The simplified equations derived in this section are validated through comparison with the explicit model of Section II, for a variety of commercially available c-Si and

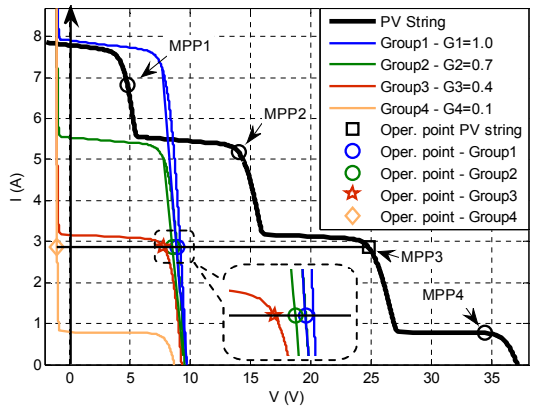

Fig. 16. *I-V* curve of a PV string comprising four cell strings, each illuminated at a different irradiance level. *I-V* curves of individual cell strings also shown in color. Focus on the operating points of individual cell strings at MPP3.

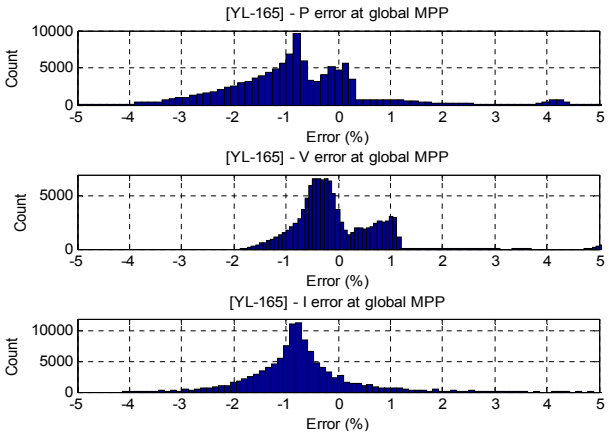

Fig. 17. Histogram of global MPP estimation errors of the simplified equations (19) applied to a study-case string of 20 PV modules (Yingli YL-165), operating at 4 irradiance levels (100 W/m^2 – 1100 W/m^2).

mc-Si PV modules. A great number of possible shading scenarios were simulated for a PV string comprising 20 modules and experiencing four irradiance levels, varying in the range of 100-1100 W/m^2 (110,606 scenarios in total). The estimation error of the simplified formulae (19) in calculating the global MPP of the entire string (P_{mp}, V_{mp}, I_{mp}) are shown in Table IV for ten indicative commercial modules (RMS and maximum errors over all examined shading scenarios). The statistical distribution of the error is presented in Fig. 17 for one example module. The overall performance of the simplified formulae is absolutely satisfactory, considering the great simplification achieved for the evaluation of the MPP, using only datasheet information. RMS errors are lower than 2% in all cases, while the maximum errors recorded (up to 9%) correspond to extreme shading scenarios.

VI. Conclusion

In this paper, an explicit PV string model using the Lambert W function was introduced, which combines the versatility and accuracy provided by the one-diode model with a significantly faster and more robust execution, intended to be used for energy yield calculations and PV system analysis and optimization. The proposed model was experimentally validated, at the level of a PV module and a PV string, and proved to be satisfactory in most practical situations.

The model was then used to study the operation of partially shaded PV strings, experiencing several irradiance levels, which give rise to multi-peak *P-V* characteristics. Simplified equations were introduced in the paper to estimate the multiple MPPs using only basic datasheet information, dispensing with the need to resort to laborious modeling and time-consuming simulations. The accuracy of the simplified equations is proved to be quite satisfactory, permitting quick and reliable estimation of partial shading effects on a PV string.

TABLE IV
Error of Global MPP Estimation using the Simplified Formulae (19), for a PV string consisting of various commercial PV modules, operating at 4 irradiance levels

PV modules	P_{mp} error (%)		V_{mp} error (%)		I_{mp} error (%)	
	RMS	MAX	**RMS**	MAX	**RMS**	MAX
Yingli YL-165	**1.60**	8.03	**1.00**	5.45	**1.19**	7.29
Aleo s18-235	**1.66**	8.58	**1.22**	4.02	**0.69**	5.73
Suntech STP 280-24/Vd	**1,53**	7,20	**1,28**	2,93	**0,67**	4,97
Conergy PH 240P	**1.69**	8.56	**1.17**	4.05	**0.80**	6.61
Upsolar UP-M240P	**1.28**	8.32	**0.92**	4.16	**0.67**	5.70
Siliken SLK60P6L	**1.28**	8.32	**0.92**	4.16	**0.67**	5.70
Bosch M60-245	**1.50**	8.17	**1.05**	3.75	**0.71**	5.46
Suntech STP240s	**1.26**	7.51	**0.97**	5.04	**0.63**	4.83
Sunpower E19/240	**1.11**	5.66	**0.92**	4.63	**0.52**	3.50
Upsolar UP-M205M	**1.30**	6.55	**1.03**	3.19	**0.60**	5.11

Appendix

The Lambert W function $W\{x\}$ is the inverse of the equation $W \cdot e^W = x$, and in the last decades has found many applications in pure and applied mathematics [29]-[33]. It cannot be expressed in terms of elementary functions, so computational environments such as *Matlab*© use iterative algorithms to provide generalized calculation of all complex branches at machine's accuracy. However, when focused on the main branch W_0 at positive real values, several series expansions may be found in the literature, each one convergent at certain ranges. Here, an asymptotic formula for moderate and large real values is chosen [29], combined with a series expansion accurate at small values [34], and formulated with the appropriate number of terms so that the relative error is maintained below 0.1%:

For $0 \le x \le 9$:

$$W = u + \frac{u}{1+u} p + \frac{1}{2} \frac{u}{(1+u)^3} p^2 - \frac{1}{6} \frac{u(2u-1)}{(1+u)^5} p^3 + \frac{1}{24} \frac{u(6u^2-8u+1)}{(1+u)^7} p^4 - \frac{1}{120} \frac{u(24u^3-58u^2+22u-1)}{(1+u)^9} p^5 \quad (20)$$

where $u=x/e$ and $p=1-x/e$.

For $x \ge 9$:

$$W = L_1 - L_2 + \frac{L_2}{L_1} + \frac{L_2(-2+L_2)}{2L_1^2} + \frac{L_2(6-9L_2+2L_2^2)}{6L_1^3} + \frac{L_2(-12+36L_2-22L_2^2+3L_2^3)}{12L_1^4} + \frac{L_2(60-300L_2+350L_2^2-125L_2^3+12L_2^4)}{60L_1^5} \quad (21)$$

where $L_1=\ln(x)$ and $L_2=\ln(\ln(x))$.

REFERENCES

[1] W. De Soto, S.A. Klein, and W.A. Beckman, "Improvement and validation of a model for photovoltaic array performance", *Solar Energy*, vol. 80, pp. 78-88, 2006.

[2] H. Tian, F. Mancilla-David, K. Ellis, E. Muljadi, and P. Jenkins, "A cell-to-module-to-array detailed model for photovoltaic panels", *Solar Energy*, in press, 2012.

[3] D. L. King,W. E. Boyson, and J.A.Kratochvil. (2004). "*Photovoltaic Array Performance Model*" [Online]. Available: http://photovoltaics. sandia.gov.

[4] W. Zhou, H. Yang, and Z. Fang, "A novel model for photovoltaic array performance prediction", *Applied Energy*, vol. 84, pp. 1187-1198, 2007.

[5] W. Durisch, B. Bitnar, J. Maylor, H. Kiess, K. Lam, and J. Close, "Efficiency model for photovoltaic modules and demonstration of its application to energy yield estimation", *Solar Energy Materials & Solar Cells*, vol. 91, pp. 79-84, 2007.

[6] V. Quaschning, and R. Hanitsch, "Numerical simulation of current-voltage characteristics of photovoltaic systems with shaded solar cells", *Solar Energy*, vol. 56, no. 6, pp.513-520, 1996.

[7] G. Liu, S. K. Nguang, and A. Partridge, "A general modeling method for I-V characteristics of geometrically and electrically configured photovoltaic arrays", *Energy Conversion and Management*, vol. 52, pp. 3439-3445, 2011.

[8] E. Karatepe, M. Boztepe, and M. Colak, "Development of a suitable model for characterizing photovoltaic arrays with shaded solar cells", *Solar Energy*, vol. 81, pp. 977-992, 2007.

[9] D. D Nguyen, and B. Lehman, "Modeling and Simulation of Solar PV Arrays under Changing Illumination Conditions", *2006 IEEE COMPEL Workshop*, Rensselaer Polytechnic Institute, Troy, NY, USA, July 2006, pp. 295-299.

[10] H. Patel, and V. Agarwal, "MATLAB-Based Modeling to Study the Effects of Partial Shading on PV Array Characteristics", *IEEE Transactions on Energy Conversion*, vol.23, no.1, pp. 302-310, March 2008.

[11] G. Petrone, and C.A. Ramos-Paja, "Modeling of photovoltaic fields in mismatched conditions for energy yield evaluations", *Electric Power Systems Research*, vol. 81, pp. 1003-1013, 2011.

[12] E. Paraskevadaki, and S. Papathanassiou, "Evaluation of MPP Voltage and Power of mc-Si PV Modules in Partial Shading Conditions", *IEEE Transactions on Energy Conversion*, vol. 26, no. 3, pp. 923-932, 2011.

[13] F. Martinez-Moreno, J. Munoz, and E. Lorenzo, "Experimental model to estimate shading losses on PV arrays", *Solar Energy Materials & Solar Cells*, vol. 94, pp. 2298-2303, 2010.

[14] J. Ding, and R. Radhakrishnan, "A new method to determine the optimum load of a real solar cell using the Lambert W-function", *Solar Energy Materials & Solar Cells*, vol. 92, pp. 1566-1569, 2008.

[15] A. Jain, and A. Kapoor, "A new approach to study organic solar cells using Lambert W-function", *Solar Energy Materials & Solar Cells*, vol. 86, pp. 197-205, 2005.

[16] G. Petrone, G. Spagnuolo, and M. Vitelli, "Analytical model of mismatched photovoltaic fields by means of Lambert W-function", *Solar Energy Materials & Solar Cells*, vol. 91, pp. 1652-1657, 2007.

[17] D. Picault, B. Raison, S. Bacha, J. de la Casa, and J. Aguilera, "Forecasting photovoltaic array power production subject to mismatch losses", *Solar Energy*, vol. 84, pp. 1031-1309, 2010.

[18] M.L. Orozco-Gutierrez, J.M. Ramirez-Scarpetta, G. Spagnuolo, and C.A. Ramos-Paja, "A technique for mismatched PV array simulation", *Renewable Energy*, vol. 55, pp. 417-427, 2013.

[19] J. D. Bastidas, E. Franco, G. Petrone, C.A. Ramos-Paja, and G. Spagnuolo, "A model of photovoltaic fields in mismatching conditions featuring an improved calculation speed", *Electric Power Systems Research,* vol. 96, pp. 81-90, 2013.

[20] Z. Salam, K. Ishaque, and H. Taheri, "An Improved Two-Diode Photovoltaic (PV) Model for PV System", *Power Electronics, Drives and Energy Systems (PEDES) & 2010 Power India*, 2010 Joint International Conference on, pp. 1-5, 2010.

[21] M.C. Alonso-Garcia, and J.M. Ruiz, "Analysis and modeling the reverse characteristic of photovoltaic cells", *Solar Energy Materials & Solar Cells*, vol. 90, pp. 1105-1120, 2006.

[22] H. Kawamura, K. Naka, N. Yonekura, S. Yamanaka, H. Kawamura, H. Ohno, and K. Naito, "Simulation of I-V characteristics of a PV module with shaded PV cells", *Solar Energy Materials & Solar Cells*, vol. 75, pp. 613-621, 2003.

[23] J.W. Bishop, "Computer simulation of the effects of electrical mismatches in photovoltaic cell interconnection circuits", *Solar Cells*, vol. 25, pp. 73-89, 1998.

[24] S.L. Miller, "Ionization Rates for Holes and Electrons in Silicon", *Physical Review*, vol. 105, pp. 1246-1249, 1957.

[25] S. Silvestre, and A. Chouder, "Effects of Shadowing on Photovoltaic Module Performance", *Progress in Photovoltaics: Research and Applications,* vol. 16, pp. 141-149, 2008.

[26] S. Silvestre, A. Boronat, and A. Chouder, "Study of bypass diodes configuration on PV modules", *Applied Energy,* vol. 86, pp. 1632-1640, 2009.

[27] M. Abramowitz, I.A. Stegun, Solutions of quartic equations, Par. 3.8.3, in: "*Handbook of Mathematical Functions with Formulas, Graps and Mathematical Tables*", Dover, New York, 1972, pp. 17_18. 9th printing.

[28] Quartic function [Online]. Available: http://en.wikipedia.org/wiki/Quartic_function.

[29] R. Corless, G. Gonnet, D. Hare, D. Jeffrey, and D. Knuth, "On the Lambert W Function", *Adv. Comput. Math*, vol. 5, no. 4, pp. 329-359, 1996.

[30] Lambert W function [Online]. Available: http://en.wikipedia.org/wiki/Lambert_W_function.

[31] C.T. Goundar, "An Explicit Solution for Progress Curve Analysis in Systems Characterized by Endogenous Substrate Production", *Microbial Ecology,* vol. 63, pp. 898-904, 2012.

[32] L. Zhang, D. Xing, and J. Sun, "Calculation activation energy of amorphous phase with the Lambert W function", *Journal of Thermal Analysis and Calorimetry,* vol. 100, pp. 3-10, 2010.

[33] A.H. Hu, Y.P. Zhao, Y.J. Guo, and M.Y. Zheng, "Analysis of linear resisted projectile motion using the Lambert W function", *Acta Mechanica,* vol. 223, pp. 441-447, 2012.

[34] R. Corless, D. Jeffrey, and D. Knuth, "A Sequence of Series for The Lambert W Function", *ISSAC '97*, pp. 1-10, 1997.

BIOGRAPHIES

Efstratios I. Batzelis (SM'13) received the Diploma in Electronic & Computer Engineering from the Technical University of Crete (TUC), Chania, Greece, in 2009, and his M.Sc. degree on Energy Production & Management from the National Technical University of Athens (NTUA), Athens, Greece, in 2012, where he is currently working towards the Ph.D. degree. His current research interests include renewable energy technologies, especially photovoltaic system design and simulation under mismatched operation.

Iason A. Routsolias (SM'13) received the Diploma in Electrical & Computer Engineering from the National Technical University of Athens (NTUA), Athens, Greece, in 2008. Currently he is working towards the Ph.D. degree. His research interests lie in the field of renewable energy generation, especially energy yield estimation in PV plants. He has worked for the Public Power Corporation of Greece, where he was involved in the connection of RES stations to the distribution network.

Stavros A. Papathanassiou (S'93–M'98–SM'10) received the Diploma degree in electrical engineering and the Ph.D. degree from the National Technical University of Athens (NTUA), Athens, Greece, in 1991 and 1997, respectively. He was with the Distribution Division of the Public Power Corporation of Greece, engaged in power quality and DG studies. In 2002, he joined the Electric Power Division of NTUA, where he is currently an Associate Professor. His research interests are in the field of RES and DG, including wind turbine and PV technology, storage applications and integration of DG to the grid. In 2009-2012 he was a Member of the Board of the Hellenic Transmission System Operator. Dr. Papathanassiou is a member of CIGRE.